



A Novel and Freely Available Interactive 3d Model of the Internal Carotid Artery

Marc Valera-Melé¹ · Anna Puigdemívol-Sánchez^{1,2}  · Marija Mavar-Haramija¹ · Juan A. Juanes-Méndez³ · Luis San-Román⁴ · Matteo de Notaris⁵ · Alberto Prats-Galino¹

Received: 28 November 2017 / Accepted: 19 February 2018
© Springer Science+Business Media, LLC, part of Springer Nature 2018

Abstract

We describe a new and freely available 3D interactive model of the intracranial internal carotid artery (ICA) and the skull base that also allows to display and compare its main segment classifications. High-resolution 3D human angiography (isometric voxel's size 0.36 mm) and Computed Tomography angiography images were exported to Virtual Reality Modeling Language (VRML) format for processing in a 3D software platform and embedding in a 3D Portable Document Format (PDF) document that can be freely downloaded at <http://diposit.ub.edu/dspace/handle/2445/112442> and runs under Acrobat Reader on Mac and Windows computers and Windows 10 tablets. The 3D–PDF allows for visualisation and interaction through JavaScript-based functions (including zoom, rotation, selective visualization and transparentisation of structures or a predefined sequence view of the main segment classifications if desired). The ICA and its main branches and loops, the Gasserian ganglion, the petrolingual ligament and the proximal and distal dural rings within the skull base environment (anterior and posterior clinoid processes, silla turcica, ethmoid and sphenoid bones, orbital fossae) may be visualized from different perspectives. This interactive 3D–PDF provides virtual views of the ICA and becomes an innovative tool to improve the understanding of the neuroanatomy of the ICA and surrounding structures.

Keywords 3D–PDF document, Internal carotid artery segments · Anatomic models · Skull base anatomy · CT angiography · 3D angiography

Introduction

Three-dimensional (3D) models may be embedded in portable document format (PDF) files that may be opened in any freely

available Adobe® Acrobat Reader® in desktop computers, allowing interactive visualization (zoom, rotation, selection of components) being of scholar and clinical interest for exploring complex biomedical data [1].

That technology has already been used to develop 3D models in biology [2, 3]. Human models exist in different fields such as fossil hominin specimens [4], a 3D atlas of the developing human embryo [5], anatomical models of the pelvis [6, 7] or for routine medical reporting to display various resection proposals for liver surgery [8]. Our group has previously produced 3D–PDF models to enhance clinicians' anatomical and neurosurgical understanding of different regions of the skull base [9, 10] and of endonasal approaches to the ICA [11–14], or structures involved in neuraxial anesthesia [15]. We have now used that technology to assess the ICA anatomy and have created a new interactive 3D–PDF model based on human neuroimages.

The internal carotid artery (ICA) extends from the bifurcation of the common carotid artery (CCA) in the neck to its final intracranial bifurcation where it divides into the middle cerebral artery (MCA) and anterior cerebral artery (ACA).

This article is part of the Topical Collection on *Education & Training*

✉ Anna Puigdemívol-Sánchez
apuigdemívol@ub.edu

- ¹ Laboratory of Surgical Neuroanatomy, Human Anatomy and Embryology Unit, Faculty of Medicine and Health Sciences, University of Barcelona, c/ Casanova 143, 08036 Barcelona, Spain
- ² CAP Antón Borja, Consorci Sanitari de Terrassa, c/ Edison s/n, 08191 Rubí, Spain
- ³ VisualMed System Group, Human Anatomy and Histology Department, University of Salamanca, Av Alfonso X el Sabio s/n, 37007 Salamanca, Spain
- ⁴ Clinic Center of Diagnostic by Imaging –Angioradiology–, Hospital Clinic, c/ Villarroel 170, 08036 Barcelona, Spain
- ⁵ Neurosurgical Department, G Rummo Hospital, Via Pacevecchia 53, 82100 Benevento, Italy

Many authors have described the course of the ICA from different perspectives of its morphology and loops [16] and proposed classifications [17–20] with different numbers of segments.

The aim of this study is to describe a new tool to understand the 3D anatomy of the ICA and its complex relationships with surrounding structures, which also illustrates the major classifications of ICA segments.

Material and methods

The anonymised neuroimaging scans (cranial computed tomography (CT) angiography and 3D high-resolution angiography) of a patient with an anterior communicating artery aneurysm that did not affect the anatomy of either ICA were used. Informed consent was obtained from the individual participant included in the study. The study followed the Declaration of Helsinki principles.

The methodology of this study can be divided into three main steps: (a) data acquisition, (b) image processing (segmentation and surface reconstruction) and analysis, and (c) 3D–PDF development.

Data acquisition

The cranial CT angiography images were acquired with a Siemens SOMATOM Multidetector CT Scanner (Siemens Healthcare, Erlangen, Germany) from the Neuroradiology Service of Hospital Clinic, with the following parameters: 0.6 mm of slice thickness, reconstructed every 0.4 mm, applying 120 kV and 50 ml of intravenous contrast (4 ml/s).

The 3D high-resolution angiography images were acquired with a Siemens CT Scanner (AXIOM Artis interventional angiography systems; Erlangen, Germany). The rotational study obtained by 3D angiography consisted in 133 images every 0.7 s in a 100° rotation, applying 70 kV. Then, 501 axial images (tomographic reconstructions) were obtained, with an isometric voxel size of 0.36 mm.

Image processing and analysis

Anonymised images were exported in Digital Imaging and Communications in Medicine (DICOM) format to be processed in the Laboratory of Surgical NeuroAnatomy, as described previously [9, 10]. To align these images, the angio-CT and 3D angiography were co-registered. Then, images were segmented by means of a 3D editor software designed for visualising and analysing biomedical images (Amira 5.3, Mercury Co, Boston, USA). Images were segmented in the three orthogonal planes (axial, sagittal, and coronal). Semiautomatic threshold segmentation, that discriminated the most ‘white’ voxels (skull in CT and blood vessels in 3D

angiographies), was combined with ‘region connected’ tools of the software to select the vessels with continuity to the ICA and with manual delimitation of the borders of each arterial branch, creating the volumes of interest (VOI) of the following structures: the skull base, the ICA, and the main branches of the ICA (i.e., ophthalmic artery (OphA), anterior choroidal artery (AChA), posterior communicating artery (PCoA), MCA and ACA). We also reconstructed other anatomical structures, such as the Gasserian ganglion (GG), the petrolingual ligament (PLL), and the proximal and distal dural rings, according to anatomical description (Figs. 1 and 2). The VOI of the ICA was then divided into different segments depending on each of the existing classifications and according to the descriptions of the limits of each segment.

3D–PDF development

The development of a 3D–PDF from DICOM files has been described previously [20]. Briefly, the VOIs of the ICA and of the neuroanatomical structures segmented were used to generate the corresponding 3D surface models, which were exported together with the angio-TC 2D images as Virtual Reality Model Language (VRML) documents that may be embedded in 3D–PDF files. The four classifications [17–20] were then visualised, analysed, and compared.

Results

The interface of the 3D–PDF consists of three functional areas: a control area, a 3D working area and a presentation area. The control area is on the left side of the interface (Fig. 1a) and contains buttons on the top that show the model in anterior, lateral, superior, and posterior views (Fig. 1a, blue arrow 1). Below there is a drop-down list of 3D reconstructed structures and ICA segment classifications (Fig. 1a, blue arrow 2), which we can select to make them appear on the central screen, in the 3D working area. The model displayed can be rotated in 360°, zoomed, or translated. We can selectively show or hide each structure with the button below the list, with the option of applying partial transparency effects with the adjacent vertical arrows (Fig. 1b blue arrow 3). Representative angio-CT slices are included in the three orthogonal planes (axial, sagittal and coronal), that can be displaced and visualised either independently or in combination with the other 3D structures (Fig. 1b, blue arrow 4). The models can be clipped in the three orthogonal planes in order to enhance the visualization of internal structures (Fig. 1b, blue arrow 5; Fig. 2a, c and Fig. 3c, d). Finally, there is a presentation area below the screen area; this contains controls that can reproduce a presentation with predetermined custom views (Fig. 1, blue arrow 6). When the presentation is active, a small description appears above the arrows.

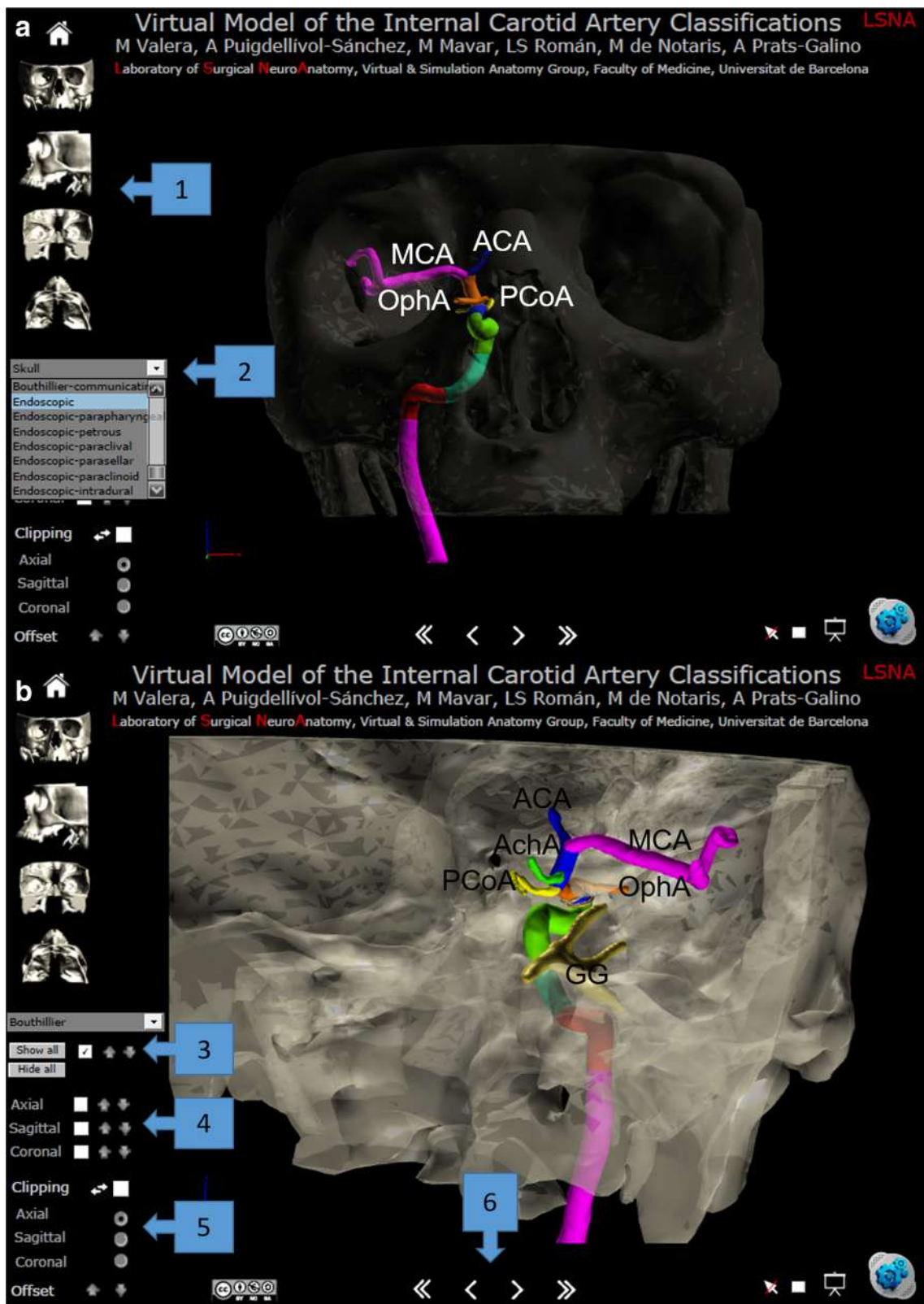


Fig. 1 The 3D-PDF interface. **a.** Endonasal perspective. 1. Anterior, lateral, posterior, and superior views. 2. Drop-down list of 3D reproduced structures. **b.** Superolateral perspective. 3. Check box to allow a specific structure to be selectively shown or hidden, with

arrows to increase or decrease transparency. 4. Selection of computed tomography slices with arrows to navigate among them. 5. Clipping and navigation in the orthogonal planes. 6. Arrows that lead to a sequence of predefined views of the different classifications

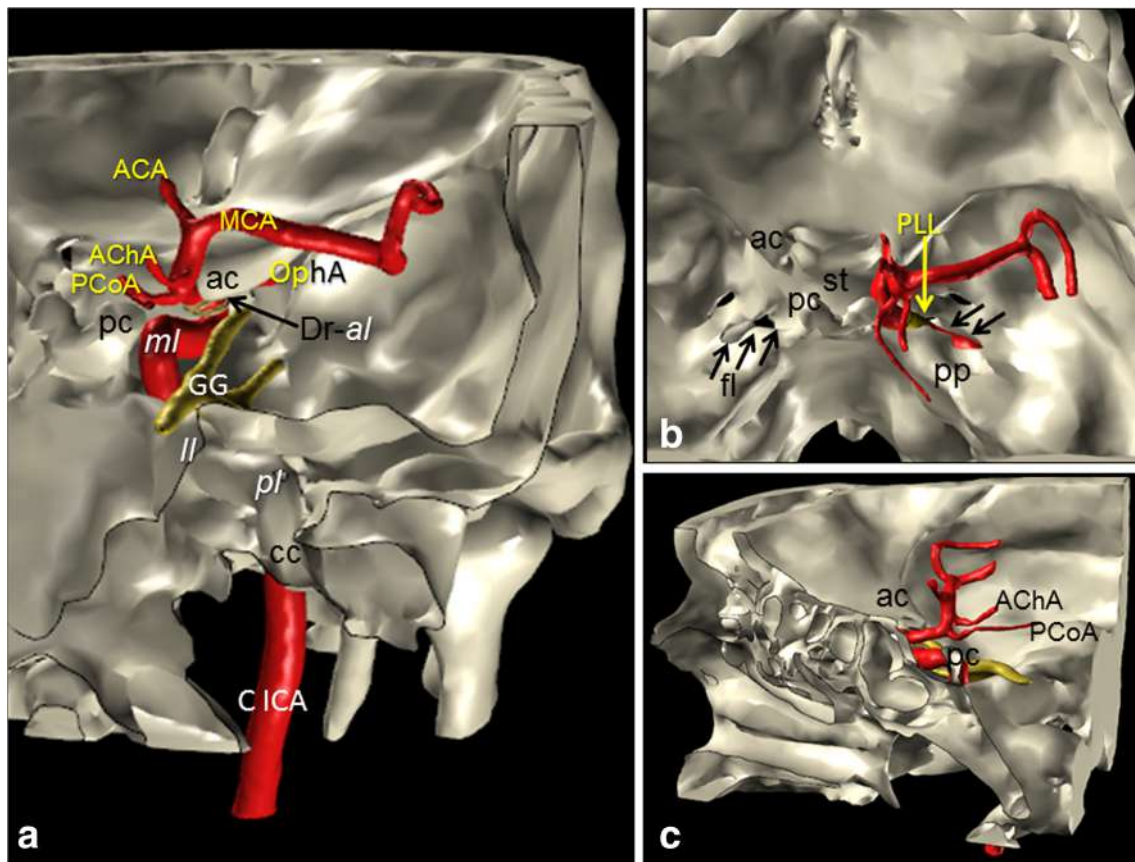


Fig. 2 ICA course. Illustrations of the relationships of the ICA with adjacent bone processes (carotid canal -cc- within the petrous pyramid -pp-, posterior clinoid -pc- and anterior clinoid -ac- processes and silla turcica -st- of the sphenoid bone) and the foramen lacerum (fl). The PLL and dural rings (Dr) are the proximal and distal limits of the cavernous sinus, respectively, while the GG is located laterally to the sinus. The ICA presents different loops (posterior -pl- within the petrous pyramid, lateral -ll- when entering the cavernous sinus, medial -ml- at the level of the posterior clinoid process -pc-, and anterior -al- below the anterior clinoid process -ac-). The main branches of the ICA (OphA, AchA and PcoA) arise before its bifurcation in ACA and MCA.

The resulting 3D–PDF document can be downloaded free of charge from a public repository hosted by the University of Barcelona (<http://diposit.ub.edu/dspace/handle/2445/112442>). It runs under Acrobat Reader (XI or superior) in Windows and Mac computers and Windows 10 tablets but not on smartphones or Linux systems. The ICA course is illustrated in Fig. 2. Corresponding segment classifications may be based on an endoscopic (Fig. 1a) or on an intracranial perspective (Fig. 1b). It may be also customized to enhance the ICA perspective in different neurosurgical approaches (Fig. 3).

Discussion

3D models obtained from cross-sectional images can be embedded in PDF files, making them a powerful tool for

a. Posterior view. Coronal clipped model at the level of the petrous pyramid to enhance the visualization of cervical ICA (C ICA) entering the carotid canal (cc) within the petrous pyramid. **b.** Superior view. ICA abandons the carotid canal and passes over the foramen lacerum (descending arrows, right side) before entering the cavernous sinus when traversing the PLL. The foramen lacerum (ascending arrows, left side) is covered by fibrocartilaginous tissue. **c.** Medial Lateral view. Sagittal clipped model at the level of the silla turcica, sphenoid sinus and ethmoidal cells. The ICA becomes subarachnoid at the level of the anterior clinoid process (ac)

clinical, educational, and research purposes [1, 22]. We have previously produced a virtual 3D–PDF model of neurosurgical related models [9–14] as well as a virtual 3D model of the lumbar spine for anaesthetic procedures [15], explaining the advantages of using the interactive and widely available free PDF format [23]. Based on this extensive experience, we are confident that our 3D–PDF prototypes of the ICA classifications provide a significant opportunity to improve the comprehension of the neuro-anatomical relations of the artery and associated vascular pathology, of interest in neurosurgery and neuroradiology. The specific anatomical details and comparison of the different segment classifications of the ICA, related to its neurosurgical interest, are analysed separately.

We believe that our methodology created an advanced 3D visual representation of this region of interest in a clinical setting (neurosurgical, neurological or neuroradiological).

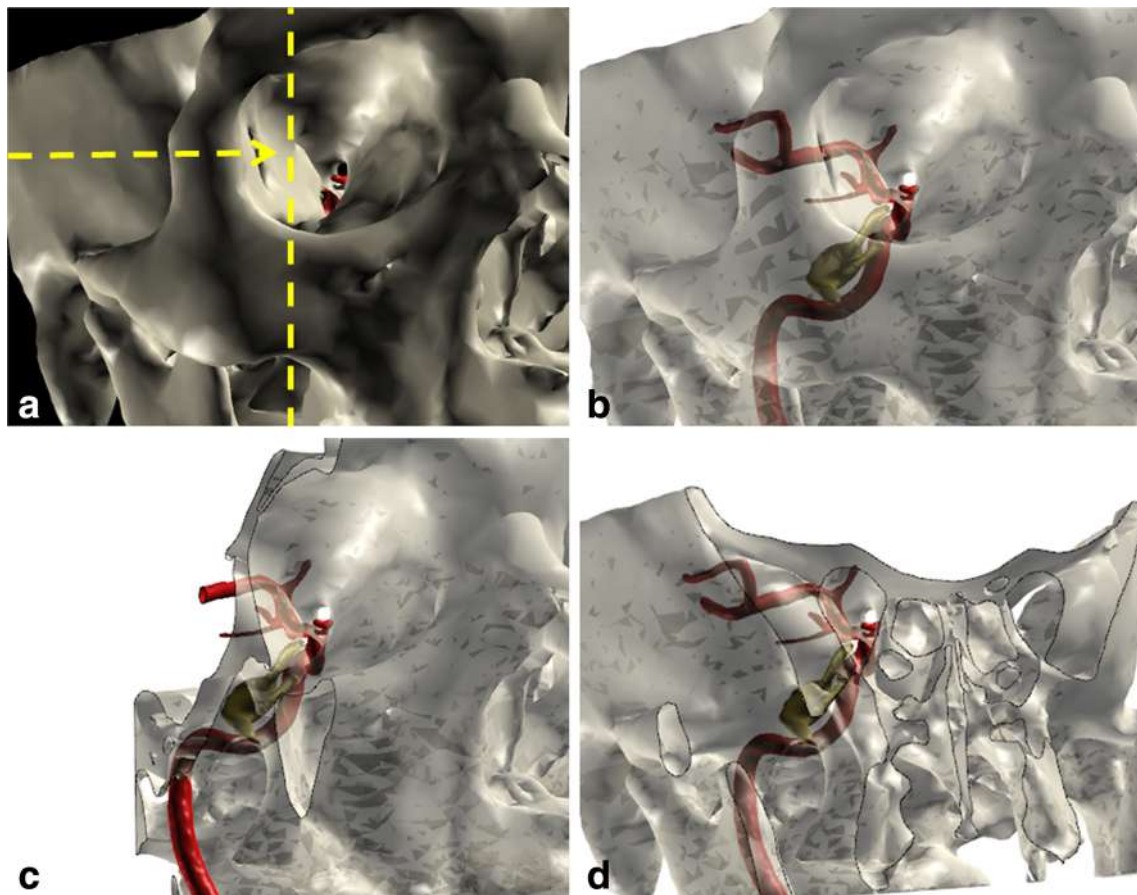


Fig. 3 3D–PDF Customization. The model may be adapted to enhance the visualization of different neurosurgical approaches. The PDF toolbar, available through the right button of the mouse, allows for effects like changing the background colour. Here, the perspective of a transorbital window [21] is simulated by means of a ventrolateral view (a), its skull

transparenciation (b), a sagittal lateral clipping to exclude the zygomatic bone (c) –at the level of the vertical discontinuous plane indicated in (a)– and a coronal clipping (d) at the level of the superior orbital fissure – horizontal plane in (a)– to enhance the visualization of the ICA in the middle cranial fossa

Indeed, the spatial perspective of the ICA is difficult to acquire with only traditional one-dimensional or two-dimensional images. So, the use of interactive 3D ICA reconstructions improves the anatomical analysis acquiring specific visual information.

Conclusion

The present study provides the first interactive and universally available 3D–PDF tool based on high-resolution angiography data to provide a new and deep approach to the knowledge of the neuroanatomy of the ICA, its surrounding structures and segment classifications.

Acknowledgements The authors are grateful to Olga Fuentes for her contribution to image processing.

Funding This study was funded by the Fundació Marató TV3 Project [411/U/2011 - TITLE: Quantitative analysis and computer aided simulation of minimally invasive approaches for intracranial vascular lesions].

Compliance with ethical standards

Conflict of interest The authors declare that they have no conflict of interest.

Informal consent Informal consent was obtained from the individual participant included in the study. All procedures were in accordance with the ethical standards of the institution and with the 1964 Helsinki declaration and its later amendments or comparable ethical standards.

References

1. Newe, A., and Becker, L., Using interactive 3D PDF for exploring complex biomedical data: experiences and solutions. *Stud Health Technol Inform* 228:740–744, 2016.
2. van de Kamp, T., dos Santos, R. T., Vagovic, P., Baumbach, T., and Riedel, A., Three-dimensional reconstructions come to life- interactive 3D PDF animations in functional morphology. *Plos One* 9: e102355, 2014.
3. Quayle, M. R., Barnes, D. G., Kaluza, O. L., and McHenry, C. R., An interactive three dimensional approach to anatomical description-the jaw musculature of the Australian laughing kookaburra (*Dacelo novaeguineae*). *PeerJ* 2:e3555, 2014.

4. Skinner, M. M., Kivell, T. L., Potze, S., and Hublin, J. J., Microtomographic archive of fossil hominin specimens from Kromdraai B, South Africa. *J Hum Evol* 64:434–447, 2013.
5. Bakker, B. S., de Jong, K. H., Hagoort, J., Oostra, R. J., and Moorman, A. F., Towards a 3-dimensional atlas of the developing human embryo: the Amsterdam experience. *Reprod Toxicol* 34: 225–236, 2012.
6. Balava, V., Uhl, J. F., Lanore, A., Salachas, C., Samoyeau, T., Ngo, C., Bensaid, C., Cornou, C., Rossi, L., Douard, R., Bats, A. S., Lecuru, F., and Delmas, V., 3D modelling of the female pelvis by computer-assisted anatomical dissection: applications and perspectives. *J Gynecol Obstet Biol Reprod (Paris)* 45:467–477, 2016.
7. Wu, Y., Dabhoiwala, N. F., Hagoort, J., Shan, J. L., Tan, L. W., Fang, B. J., Zhang, S. X., and Lamers, W. H., 3D topography of the young adult anal sphincter complex reconstructed from undermed serial anatomical sections. *PLoS One* 10:e0140736, 2015.
8. Newe, A., Becker, L., and Schenk, A., Application and evaluation of interactive 3D PDF for presenting and sharing planning results for liver surgery in clinical routine. *PLoS One* 9:e115697, 2014.
9. De Notaris, M., Palma, K., Serra, L., Enseñat, J., Alobid, I., Poblete, J., González, J. B., Solari, D., Ferrer, E., and Prats-Galino, A., A Three-dimensional computer-based perspective of the skull base. *World Neurosurg* 82:S41–S48, 2014.
10. De Notaris, M., Prats-Galino, A., Cavallo, L. M., Esposito, F., Iaconetta, G., González, J. B., Montagnani, S., Ferrer, E., and Cappabianca, P., Preliminary experience with a new three-dimensional computer-based model for the study and the analysis of skull base approaches. *Childs Nerv Syst* 26:621–626, 2010.
11. D'Avella, E., De Notaris, M., Enseñat, J., Berenguer, J., Gagnaniello, C., Mavar, M., Ferrer, E., and Prats-Galino, A., The extended endoscopic endonasal transplanum transtuberulum approach to the anterior communicating artery complex: anatomical study. *Acta Neurochir (Wien)* 157:1495–1503, 2015.
12. De Notaris, M., Prats-Galino, A., Enseñat, J., Topczewski, T., Ferrer, E., Cavallo, L. M., Cappabianca, P., and Solari, D., Quantitative analysis of progressive removal of nasal structures during endoscopic suprasellar approach. *Laryngoscope* 124:2231–2237, 2014.
13. De Notaris, M., Solari, D., Cavallo, L. M., Enseñat, J., Alobid, I., Soria, G., Gonzalez, J. B., Ferrer, E., and Prats-Galino, A., The use of a three-dimensional novel computer-based model for analysis of the endonasal endoscopic approach to the midline skull base. *World Neurosurg* 75:106–113, 2011.
14. Mavar-Haramija, M., Prats-Galino, A., Juanes-Méndez, J. A., Puigdemívol-Sánchez, A., and de Notaris, M., Interactive 3D-PDF presentations for the simulation and quantification of extended endoscopic endonasal surgical approaches. *J Med Sys* 39:127, 2015.
15. Prats-Galino, A., Mavar, M., Reina, M. A., Puigdemívol-Sánchez, A., San-Molina, J., and De Andrés, J. A., Three-dimensional interactive model of lumbar spinal structures. *Anaesthesia* 69:521, 2014.
16. Van Loveren, H. R., Keller, J. T., El-Kalliny, M., Scodary, D. J., and Tew, J. M., The Dolenc technique for cavernous sinus exploration (cadaveric prosection). *J Neurosurg* 74:837–844, 1991.
17. Fischer, E., Die lageabweichungen der vorderen hirnarterie im gefäßbild. *Zentralbl Neurochir* 3:300–313, 1938.
18. Gibo, H., Lenkey, C., and Rhoton, Jr., A., Microsurgical anatomy of the supraclinoid portion of the internal carotid artery. *J Neurosurg* 55:560–574.19, 1981.
19. Bouthillier, A., van Loveren, H. R., and Keller, J. T., Segments of the internal carotid artery: a new classification. *Neurosurgery* 38: 425–433, 1996.
20. Labib, M., Prevedello, D., Carrau, R., Kerr, E., Naudy, C., Abou Al-Shaar, H., Corsten, M., and Kasam, A., A road map to the internal carotid artery in expanded endoscopic endonasal approaches to the ventral cranial base. *Neurosurgery* 10:448–471, 2014.
21. Di Somma, A., Andaluz, N., Cavallo, L. M., de Notaris, M., Dallan, I., Solari, D., Zimmer, L. A., Keller, J. T., Zuccarello, M., Prats-Galino, A., and Cappabianca, P., Endoscopic transorbital superior eyelid approach: anatomical study from a neurosurgical perspective. *J Neurosurg* 15:1–14, 2017.
22. Phelps, A., Naeger, D. M., and Marcovici, P., Embedding 3D radiology models in portable document format. *AJR Am J Roentgenol* 199:1342–1344, 2012.
23. Prats-Galino, A., Reina, M. A., Mavar Haramija, M., Juanes Méndez, J. A., and De Andrés, J. A., 3D interactive model of lumbar spinal structures of anesthetic interest. *Clin Anat* 28:205–212, 2015.